doi: 10.17221/45/2013-RAE

Thermal and physical properties modelling of terebinth fruit (*Pistacia atlantica* L.) under solar drying

M. Kaveh[1], R. Amiri Chayjan[1], M. Esna-Ashari[2]

[1]*Department of Biosystems Engineering, Faculty of Agriculture, Bu-Ali Sina University, Hamedan, Iran*
[2]*Departments of Horticultural Sciences, Faculty of Agriculture, Bu-Ali Sina University, Hamedan, Iran*

Abstract

Kaveh M., Chayjan Amiri R., Esna-Ashari M. (2015): **Thermal and physical properties modelling of terebinth fruit (*Pistacia atlantica* L.) under solar drying**. Res. Agr. Eng., 61: 150–161.

A laboratory solar dryer was used to study terebinth fruit drying. Two solar collectors were adjusted in east-west directions with the angle of 45°. Initial moisture content of terebinth fruit was dried under natural and forced airflow. In order to predict terebinth moisture content during drying process five mathematical models were used. Colour change and shrinkage of the terebinth samples were calculated. Results showed that the Page model had the best performance in moisture content prediction of terebinth samples. Effective moisture diffusivity of terebinth fruit was increased under forced convection. The lowest colour change and shrinkage of the samples in natural air flow condition were observed. Maximum rupture force and energy values were obtained at maximum airflow velocity. Models were fitted to the experimental data of physical, thermal and mechanical properties of terebinth fruit with high correlation coefficients.

Keywords: thin layer; moisture diffusivity; shrinkage; colour; rupture energy

Drying is a complex process including simultaneous heat and mass transfer and it can result in significant changes in physical, thermal, and mechanical properties of agricultural and food materials (Koc et al. 2008). These phenomena contribute to moisture removal leading to substantial reduction in mass and volume of product, minimizing packaging, storage and transportation costs (Vega-Galvez et al. 2010). Drying kinetics of material requires simple representations to predict drying behaviour and to optimize drying parameters. Thin layer drying equations have therefore been used to predict drying time and to generalize drying curves (Arumuganathan et al. 2009).

Terebinth (*Pistacia atlantica* L.) is one of the old trees with a long life having small, round and dark green fruit with many nutritional, medicinal and industrial applications that grows in Iran. Mutica, Kurdica and Kabolica are the main terebinth cultivars that grow wild in Iran. Presence of too much moisture in fruit at harvesting time (about 116% d.b.) is a great obstacle for long term storage.

Solar drying can be considered as the development of open sun drying which an efficient method of solar energy utilization (Janjai et al. 2009). Sun drying allows the preparation of a new product presenting high quality of colour with translucent appearance. However this method has some disadvantages, as it

Supported by the Bu-Ali Sina University, Hamedan, Iran, Project No. 2104713.

doi: 10.17221/45/2013-RAE

is a time-consuming, labour-demanding and weather-dependent process greatly exposed to environmental contamination (Arslan, Ozcan 2010).

Physical, thermal and mechanical properties of terebinth fruit demand a specific design for the development of equipment and structures suitable for transporting, handling, processing and storage as well as assessing the behaviour of product quality (Manuwa, Muhammad 2011). Equipment optimization is also essential for decorticating, drying, harvesting, cleaning, grading and storage of terebinth kernel.

Due to drying of fruits and vegetables, shrinkage occurs when the viscoelastic tissue contracts into the space previously occupied by the transferred moisture (Yadollahinia et al. 2009). This phenomenon has directly been measured by a calliper or micrometer or though changes in some related parameters such as density and porosity (Arevalo-Pinedo et al. 2010; Zielinska, Markowski 2010).

Colour is one of the most important indices for acceptance of a product. It reflects the sensation of human eye, as visual examination is a common method for assessing products colour. Colour change of a product is occurred by the reaction of constituents in the food such as pigment destruction and non-enzymatic browning activated during drying process (Prachayawarakorn et al. 2004). One of the best methods of presenting describe colour of products is the usage of three colour components of red, green and blue (RGB) (Zheng et al. 2006).

Mechanical properties such as rupturing force and energy are useful information to be considered in designing the nut shelling and kernel grinding mechanisms. These properties are affected by some factors such as cultivar and moisture content. Rupture force indicates the min. required force for nut shelling and kernel grinding (Sirisomboon et al. 2007; Nazari Galedar et al. 2009). Many studies have been conducted on thin-layer drying of agricultural and food materials with solar dryer (Aktas et al. 2009; Janjai et al. 2009, 2011; Tripathy, Kumar 2009; Usub et al. 2010; Cakmak, Yildiz 2011); several reports have been published on volumetric shrinkage in biological materials (Abbasi Souraki, Mowla 2008; Hashemi et al. 2009; Janjai et al. 2010; Ghanem et al. 2012) and some researchers have reported the mechanical properties of biomaterials (Dash et al. 2008; Nazari Galedar et al. 2009; Altuntas et al. 2010; Singh et al. 2010; Manuwa, Muhammad 2011; Gharibzahedi et al. 2012).

No reports have been found in the literature regarding solar drying behaviour of terebinth fruit. In this work, drying characteristics, development of thin layer drying models for describing drying process, the effective moisture diffusivity, shrinkage, colour, rupture force and energy of terebinth fruit in a natural and forced convection solar dryer at different air flow rates have therefore been studied.

MATERIAL AND METHODS

Terebinth seed (cv. Kurdica) was supplied from the forests of Sardasht city, West Azarbaijan province, Iran, in July 2011. The samples were cleaned and stored in a refrigerator at +3 ± 1°C. Initial moisture content of the samples was 1.16 (d.b.) as determined using an oven at 70°C over 24 h (AOAC 2000). About 40 g sample was used in each experiment. Solar dryer was designed and fabricated in the Department of Biosystems Engineering, Bu-Ali Sina University, Hamedan, Iran (Fig. 1). The dryer included two solar collector, air channels, axial fan, air regulating damper and a drying chamber. The system was manufactured in such a way that it was enabled to use the solar energy at all daylight hours. When doing experiments in the East-West, two collectors were set at the angle of 45°. All experiments began at 7:35 and continued until 19:35. Heat of

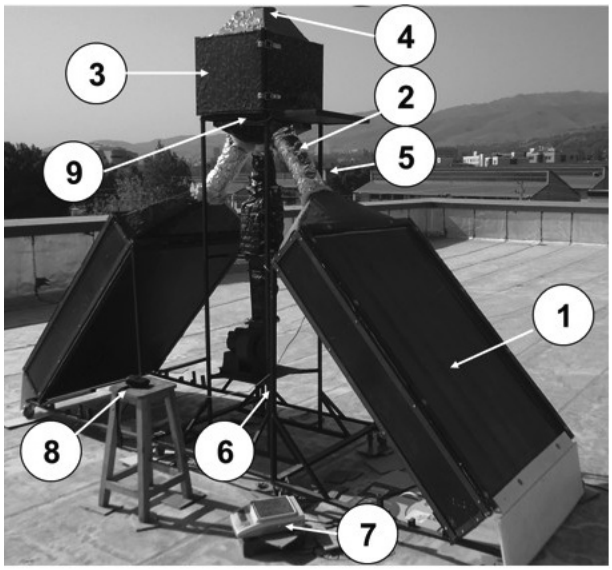

Fig. 1. Fabricated laboratory solar dryer
1 – solar collector; 2 – heat transfer duct; 3 – drying chamber; 4 – axial fan; 5 – dimmer; 6 – chasis; 7 – scale; 8 – solar power meter; 9 – thermocouple

doi: 10.17221/45/2013-RAE

Table 1. Mathematical models available applied to the drying curves

Model	Equation	References
Demir et al.	$MR = a\exp(-kt)^n + b$	Demir et al. (2007)
Logaritmic	$MR = a\exp(-kt) + c$	Usub et al. (2010)
Logestic	$MR = a/(1 + b\exp(kt))$	Cihan et al. (2007)
Page	$MR = \exp(-kt^n)$	Arslan, Ozcan (2010)
Wang and Sing	$MR = 1 + ax + bx^2$	Sacilik et al. (2006)

a, b, c, k, n – constants; MR – moisture ratio; t – time

the sun was transferred by a tube into the drying chamber and fan speed was adjusted by a dimmer for each experiment. Drying and ambient air temperatures were measured by a digital thermometer (Lutron TM-903, Lutron Electronics Co. Inc., Taipei, Taiwan) with accuracy of ± 0.1°C at one hour intervals. Drying air temperature was measured every hour by installed thermocouple at the inlet of drying chamber. Relative humidity of ambient air was also measured every hour by a hygrometer (Lutron TM-903, Taiwan) with accuracy of ± 3%. Solar radiation intensity was measured every hour by a solar power meter (Tes-1333R, TES Electrical Electronic Corp., Rui Guang, Taiwan) with accuracy of ± 10 W/m^2. Air velocity was measured by a vane type digital anemometer (Lutron AM-4202; Lutron Electronics Co. Inc., Taipei, Taiwan) with resolution of 0.1 m/s and accuracy of ± 2% at the outlet of drying chamber (Fig. 1). Final moisture content was reached at the end of each day. Experiments were conducted at three air flow rates of 0.5, 1 m/s and natural air flow. Natural air flow in the drying chamber is occurred due to heating process of air in the solar collector and flowing of it through ducts into the drying chamber. Air velocity under natural condition was very low (less than 0.1 m/s). Max. air velocity with the assembled axial fan was achieved at 1 m/s.

The moisture ratio (MR) and drying rate (DR) were calculated using the following equations during drying experiments (Usub et al. 2010; Aktas et al. 2009):

$$MR = \frac{M - M_e}{M_i - M_e} \quad (1)$$

$$DR = \frac{M_{t+dt} - M_t}{dt} \quad (2)$$

where:
MR – moisture ratio
M – moisture content (% d.b.)
M_e – equilibrium moisture content (% d.b.)
M_i – moisture content (% d.b.)
M_t – moisture content at any time (% d.b.)
t – drying time (min)
DR – the drying rate

However, the MR was simplified to M/M_i of $(M - M_e)/(M_i - M_e)$.

As terebinth fruit is a spheroid product, geometric mean diameter of the fruit can be calculated as follows (Mohsenin 1996):

$$D = (A \times B \times C)^{\frac{1}{3}} \quad (3)$$

where:
D – geometric mean diameter (m)
A, B, C – major, intermediate and minor diameters, respectively (m)

Second law of Fick for round products was presented to calculate the effective moisture diffusivity of terebinth fruit (Cakmak, Yildiz 2011). Assuming mass transfer was as diffusion mode, volume change was negligible and diffusion coefficients and temperature were constant at drying process. Moisture diffusivity can be model using the following equation (Hii et al. 2009):

$$MR = \frac{M - M_e}{M_i - M_e} = \frac{6}{\pi^2}\sum_{n=1}^{\infty}\frac{1}{n^2}\exp\left(\frac{-D_{\text{eff}}n^2\pi^2 t}{r^2}\right) \quad (4)$$

where:
n – number of terms taken into consideration
t – drying time (s)
D_{eff} – effective moisture diffusivity (m^2/s)
r – kernel radius (m)

doi: 10.17221/45/2013-RAE

For longer drying periods, Eq. (4) could be written as the first term of series only, without much effect on the prediction accuracy (Odjo et al. 2012; Amiri Chayjan et al. 2013):

$$\ln(MR) = \ln\left(\frac{M - M_e}{M_i - M_e}\right) = \ln\left(\frac{6}{\pi^2}\right) - \left(\frac{D_{\text{eff}}\pi^2 t}{r^2}\right) \quad (5)$$

then

$$MR = \left(\frac{6}{\pi^2}\right)\exp\left(-\frac{\pi^2 D_{\text{eff}} t}{r^2}\right) \quad (6)$$

The slope (K_1) is calculated by plotting ln(MR) against drying time according to Eq. (7) (Aghbashlo et al. 2009):

$$K_1 = \left(\frac{D_{\text{eff}}\pi^2}{r^2}\right) \quad (7)$$

Determination coefficient (R^2) was the primary index used to select the best model of predicting variations in the drying curves of terebinth fruit. Two statistical parameters of reduced chi-square (χ^2) and root mean square error ($RMSE$) were applied to evaluate the goodness of the models. The higher values of the determination coefficient and the lower values of the reduced chi-square and root mean square error were chosen as the criteria for goodness of fit (Usub et al. 2010). These parameters could be calculated as follow:

$$R^2 = 1 - \frac{\sum_{i=1}^{N}[MR_{\text{exp},i} - MR_{\text{pre},i}]^2}{\sum_{k=1}^{N}\left[\frac{\sum_{k=1}^{n} MR_{\text{pre},i}}{N} - MR_{\text{pre},i}\right]^2} \quad (8)$$

$$\chi^2 = \frac{\sum_{i=1}^{N}\left(MR_{\text{exp},i} - MR_{\text{pre},i}\right)^2}{N - z} \quad (9)$$

$$RMSE = \left[\frac{1}{N}\sum_{i=1}^{N}(MR_{\text{pre},i} - MR_{\text{exp},i})^2\right]^{\frac{1}{2}} \quad (10)$$

where:

$MR_{\text{exp},i}$ – experimental moisture ratio of i^{th} data

N – number of observations

z – number of drying constants

The experimental moisture content of terebinth fruit were fitted with five semi-theoretical and theoretical thin layer drying models (Table 1). Model constants were arrived using non-linear least squares regression method of the Curve Expert (Version 1.4) software between moisture ratio (MR) and drying time (t).

Shrinkage is usually defined as the sample volume change to initial volume of the drying sample. Many researchers have expressed shrinkage as a function of selected dimension changes of the samples (Desmorieux et al. 2010). Terebinth fruit volume before drying (initial volume) was computed from the following equation:

$$V_0 = \frac{4}{3}\pi\left(\frac{D}{2}\right)^3 \quad (11)$$

where:

V_0 – initial volume before drying (m^3)

D – geometric mean diameter (m)

Shrinkage of the samples was calculated using the following equation (Mercier et al. 2011):

$$S_b = \frac{(V_0 - V)}{V_0} \times 100 \quad (12)$$

where:

S_b – shrinkage (%)

V – secondary volume after drying (m^3)

Colour change (ΔRGB) of terebinth, before and after drying, was measured by the colour analyser RGB-1002 (Lutron Electronics Co. Inc., Taipei, Taiwan). Firstly, the colour analyser was calibrated using a standard calibration plate with a white surface for R (red), G (green) and B (blue). Colour change in ΔRGB is achieved using the following equations:

$$\Delta R = \frac{R_1 - R_2}{R_1} \times 100 \quad (13)$$

$$\Delta G = \frac{G_1 - G_2}{G_1} \times 100 \quad (14)$$

$$\Delta B = \frac{B_1 - B_2}{B_1} \times 100 \quad (15)$$

where:

ΔR, ΔG, ΔB – change in red, green and blue colour (%)

R_1, G_1, B_1 – red, green and blue colours before drying

R_2, G_2, B_2 – red, green and blue colours after drying

doi: 10.17221/45/2013-RAE

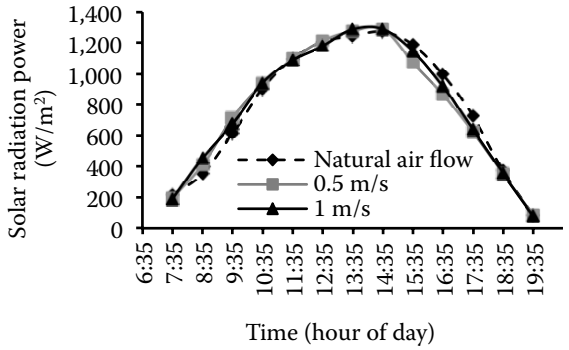

Fig. 2. Variations of solar radiation power with the drying hours of experiment days

Grain fracture point is specified with increased deformation rate as well as reduced power in the force-deformation curve and finally the body is broken. Both in hard and soft materials, a substantial transformation occur after rupture. Thus, the max. force is recorded in seed failure point on the force-deformation curve. The required energy for grain fracture is total area under force-deformation curve. Testing data to calculate the area under the curve were transferred to Microsoft Excel software. Area under the curve was calculated using the trapezoidal method. Given that, the area is equal to the energy. So, relatively much energy was needed to crack the terebinth fruit. Material testing machine (ZwickiLine 109; Zwick GmbH & Co., Ulm, Germany) was used to carry out the experiments.

RESULTS AND DISCUSSION

Variations of the ambient air solar radiation during the experiments are shown in Fig. 2 for a typical day of July 2011 in Hamedan, Iran. During the drying experiments, the daily mean values of ambient solar radiation ranged from 81–1,292 W/m^2. Morning sun radiation power was gradually increased to reach a peak. Ambient solar radiation was reached the highest values between 12:35 and 15:35. Solar radiation was gradually decreased until afternoon testing. There was also a slight random fluctuation in solar radiation. However, the overall patterns in solar radiation were sinusoidal with a sharp peak at about 14:35.

Variations of the ambient air temperature, relative humidity and temperature of the drying chamber were recorded during the experiments (Fig. 3). During the drying experiments, the daily mean values of ambient air temperature and relative humidity and drying chamber temperature ranged from 22.94 to 38°C, 9.52 to 39.7% and 24.8 to 64°C, respectively. The ambient air and drying chamber temperatures reached the highest values at about

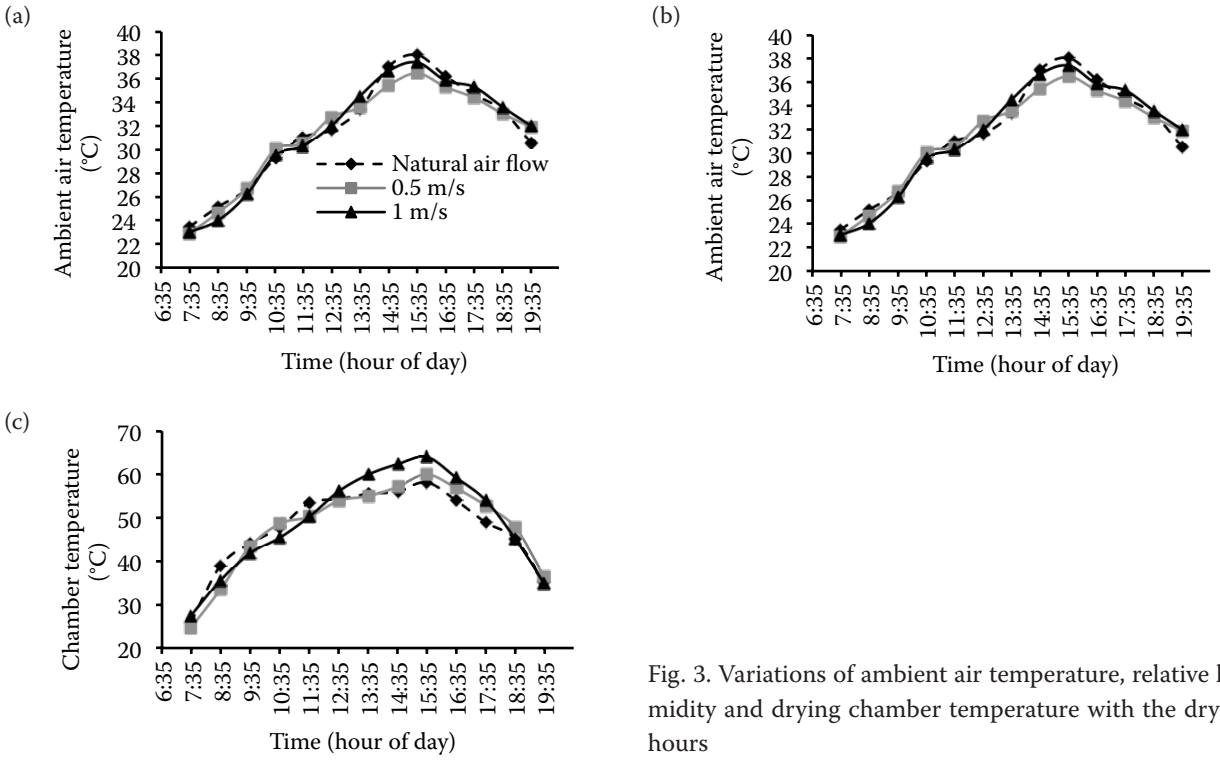

Fig. 3. Variations of ambient air temperature, relative humidity and drying chamber temperature with the drying hours

doi: 10.17221/45/2013-RAE

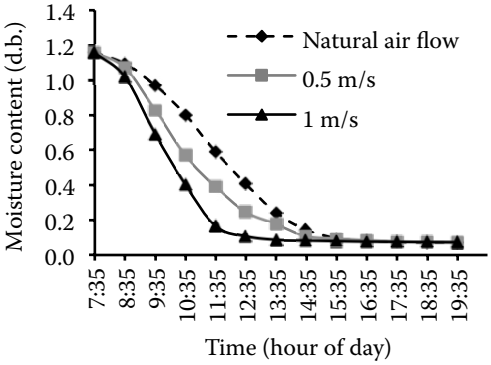

Fig. 4. Changes in moisture content versus time (hours of day) in solar drying of terebinth fruit

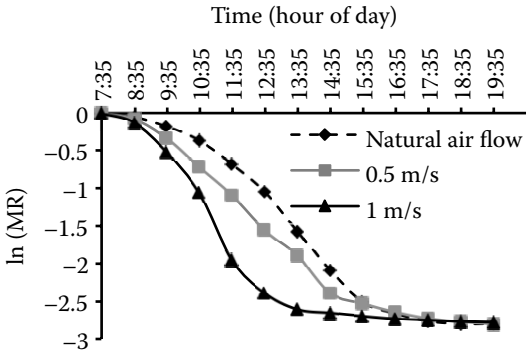

Fig. 5. Changes of lnMR versus time (hours of day) in solar drying of terebinth fruit

15:35, whereas the relative humidity was reached the lowest value during this time. Relative humidity was decreased over time at different locations inside the dryer during the first half of the day. This is caused by decreasing relative humidity of the ambient air and increasing water holding capacity of the drying air due to temperature increase, whereas the opposite is occurred for the latter half of the day. No significant differences were found between relative humidity of different positions inside the dryer. Similar results have been obtained in solar drying of tomato (Sacilik et al. 2006), banana (Janjai et al. 2009) and pepper (Hossain, Bala 2007).

Variations in the moisture content of terebinth fruit with respect to the drying time in solar dryer and three different air velocities (natural airflow, 0.5 and 1 m/s) are shown in Fig. 4. As air velocity increased, the difference between the max. entrance temperatures of the dryer chamber increased at the mid-day, and at the same time a rapid decrease in the moisture content were observed. In addition, relative humidity of the drying chamber decreased due to the higher air velocity, and therefore, vapour pressure of the drying chamber was decreased. Thus, drying time was decreased when an axial fan was placed at the exit of the dryer chamber. With increasing air velocity at the starting hours of the process, dryer chamber temperature was decreased related to air flow rate. But, with increasing solar power at the mid-day, forced convection lead to more increase in chamber temperature. Similar results have been shown in the process of drying Tila-

Table 2. Calculated effective moisture diffusivity (D_{eff}) for terebinth fruit drying

Air velocity (m/s)	D_{eff} (m^2/s)	R^2
Natural airflow	1.02×10^{-10}	0.97
0.5	1.115×10^{-10}	0.96
1	1.248×10^{-10}	0.96

R^2 – correlation coefficients, D_{eff} – effective moisture diffusivity

Table 3. Modelling of moisture ratio versus drying time for terebinth fruit at different drying conditions

Model	Air velocity (m/s)	R^2	χ^2	*RMSE*
Demir et al.	natural airflow	0.9645	0.0597	0.2002
	0.5	0.9737	0.0374	0.1609
	1	0.9585	0.0562	0.1972
Logaritmic	natural airflow	0.9645	0.0579	0.2110
	0.5	0.9737	0.0374	0.1696
	1	0.9585	0.0562	0.2078
Logestic	natural airflow	0.9966	0.0054	0.0645
	0.5	0.9892	0.0153	0.1084
	1	0.9800	0.0271	0.1442
Page	natural airflow	0.9921	0.0094	0.0894
	0.5	0.9842	0.0147	0.1115
	1	0.9795	0.0276	0.1530
Wang and Sing	natural airflow	0.9655	0.0563	0.2182
	0.5	0.9820	0.0256	0.1471
	1	0.9540	0.0622	0.2295

RMSE – root mean square error; χ^2 – chi-square; R^2 – correlation coefficients

doi: 10.17221/45/2013-RAE

Table 4. Constant values for the Logistic model

Air velocity (m/s)	*a*	*b*	*k*
Natural airflow	1.12	0.105	0.605
0.5	1.42	0.374	0.518
1	1.20	0.176	0.869

pia fish (Kituu et al. 2010), silkworm pupae (Usub et al. 2010), seeded grape (Cakmak, Yildiz 2011) and jackfruit (Chowdhury et al. 2011).

Fig. 5 shows the ln(*MR*) versus the drying time at three different air velocities (natural airflow, 0.5 and 1 m/s). Input air velocity plays an important role in drying kinetic. More increase in input air velocity, cause increase in mass transfer and drying process can be conducted faster; therefore the slope of drying curve increases with increasing in input air velocity. The impacts of air velocity on the effective moisture diffusivity have been shown in Table 2.

The effective moisture diffusivity of terebinth fruit was found to be ranged between 1.02×10^{-10} and 1.248×10^{-10} m^2/s. These values meet the standard range (from 10^{-11} to 10^{-9} m^2/s) for food and agricultural products (Aghbashlo et al. 2009). The terebinth samples with 1 m/s, effective moisture diffusivity had the highest value compared to the other samples. Min. value of D_{eff} (1.02×10^{-10} m^2/s) achieved at the natural air flow. The value of D_{eff} for the the velocity of 1 m/s in solar drying method was higher than that of the other velocities indicating that air velocity of 1 m/s solar drying process had better mass transfer efficiency than natural solar drying at low temperatures. Results indicated that with increasing air velocity, D_{eff} value was increased. This can be attributed to the forced convection during solar drying process. Sacilik et al. (2006) reported that the effective moisture diffusivities of tomato for solar tunnel and open sun drying process were found to be 1.31×10^{-9} and 1.07×10^{-9} m^2/s, respectively. Similar results have been obtained in solar drying mulberry (Doymaz 2004), potato (Tripathy, Kumar 2009), silkworm (Usub et al. 2010) and grape seeds (Cakmak, Yildiz 2011). The following model is proposed to describe D_{eff} of the terebinth fruit in solar dryer:

$$D_{eff} = 2 \times 10^{-11} v + 1 \times 10^{-10}, R^2 = 0.9871 \quad (16)$$

where:

v – airflow velocity (m/s)

The best model for describing terebinth fruit drying was Logestic, because its correlation coefficients (R^2) was the highest and χ^2 and *RMSE* values were the lowest. R^2, χ^2 and *RMSE* values of the applied models are given in Table 3 for the terebinth samples dried at different air velocities (0.5, 1 m/s

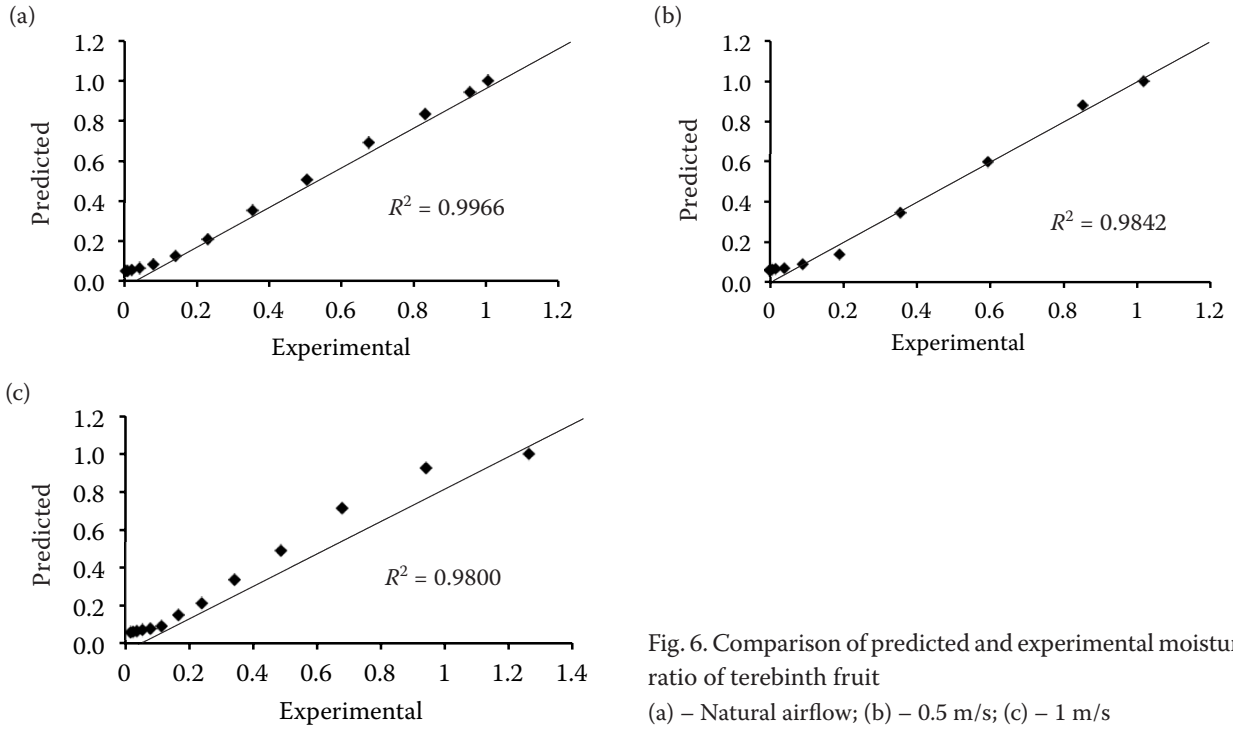

Fig. 6. Comparison of predicted and experimental moisture ratio of terebinth fruit

(a) – Natural airflow; (b) – 0.5 m/s; (c) – 1 m/s

doi: 10.17221/45/2013-RAE

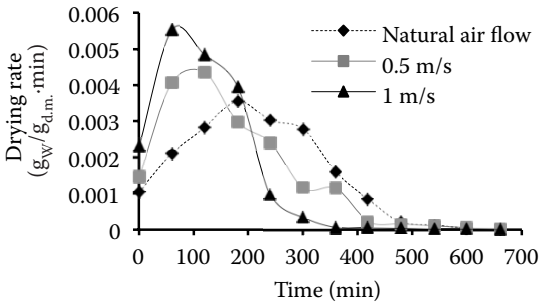

Fig. 7. Variation in drying rate according to drying time of terebinth fruit

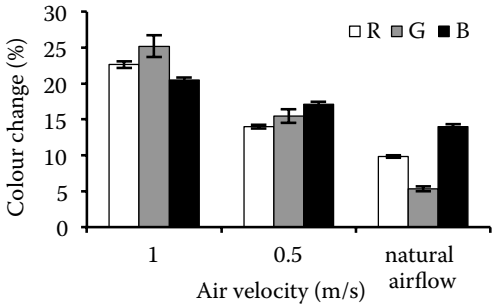

Fig. 9. Colour changes of terebinth fruit at different air velocities

and natural airflow). The average values of R^2, χ^2 and *RMSE* of the Logestic model for terebinth fruit drying were 0.9886, 0.0159 and 0.1057, respectively. Therefore, moisture ratio variation with respect to time is truly explained with this model. Cakmak and Yildiz (2011) described the drying behaviour of grapes with Midilli model (R^2= 0.9999 and χ^2= 3.4 × 10^{-9}). Coefficients of Logestic model for solar drying of terebinth fruit are shown in Table 4.

Fig. 6 shows the prediction results of the Logestic model against experimental values at different air velocities. Results proved that the predicted values by the optimized Logestic model had the suitable fitness with the experimental values. The R^2 values between predicted and experimental values for natural airflow, 0.5 and 1 m/s were achieved 0.9966, 0.9892 and 0.9800, respectively.

Fig. 7 shows drying rate (*DR*) versus drying time and the variations of drying rate with moisture content samples at drying conditions with natural airflow, 0.5 and 1 m/s. After an initial period of sample heating, drying rate reached to its max. value and then the product dried in the falling rate period. Mass transfer process initially occurred at the surface of terebinth fruit and loses relevance at subsequent stages. Drying rate is significantly affected by airflow velocity. Each drying rate curve is characterized by a distinct heating phase and a rapid initial increase in the drying rate followed by two phases with a falling rate. The sharp decrease in the drying rate curve observed during the first drying phase may suggest that neither internal nor external resistances of mass transfer dominated over this period. It may result from the appearance of free water on the surface of fruit, which increases the cohesiveness of the bed and considerably makes the spouting difficult. After a short period of drying, free water was evaporated, the height of the curve reached max. value and the drying rate was also maximal. Same results have been obtained by Doymaz (2005) in fig, Kaya et al. (2007) in apple and Hii et al. (2009) in cocoa.

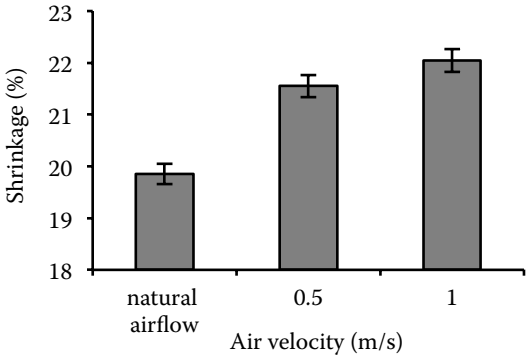

Fig. 8. Variations of shrinkage versus different air velocities for terebinth fruit

In order to determine the changes in volume of the drying samples, the dimension of the samples in three directions were measured by means of a digital calliper (SKU 8372062; Pro Tool Point Inc., Lake Forest, USA) (0–150 mm). Fig. 8 shows the variations of shrinkage (V_0 – V/V_0) versus airflow velocity of natural airflow, 0.5 and 1 m/s. Shrinkage percentage in terebinth fruit is shown in Fig. 8. Maximum value of shrinkage (22%) was calculated at airflow of 1 m/s and the lowest (19%) was achieved at natural airflow. The results indicated that increasing airflow velocity leads to the increment of the shrinkage value. According to Fig. 8, a clear impact of air velocity on samples shrinkage was observed. If rapid drying rate conditions are used and intense moisture gradients through the material are observed, low moisture content of the external surface may induce a rubber-glass transition and the formation of a porous outer rigid crust or shell that fixes the volume and complicates sub-

doi: 10.17221/45/2013-RAE

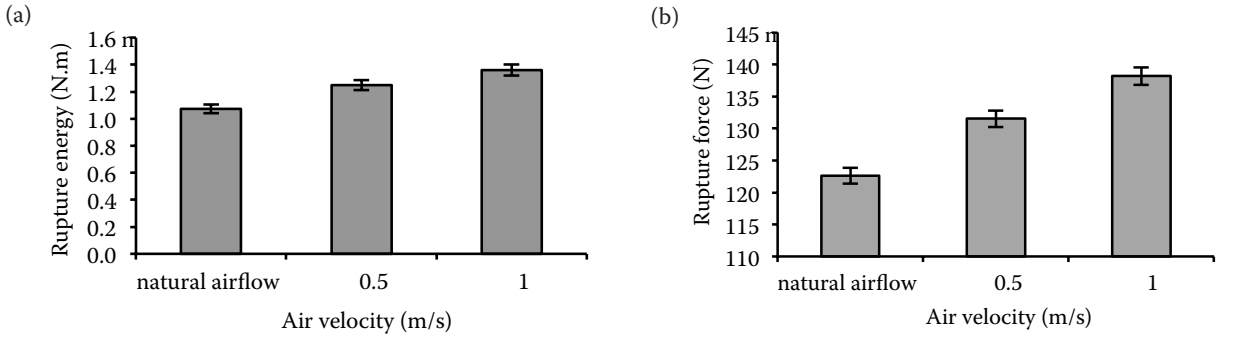

Fig. 10. Effect of (a) air velocity on rupture force and (b) energy of terebinth fruit

sequent shrinkage of the still rubbery inner part of the food. Similar results have been obtained in ber (Kingsly et al. 2007), papaya (Kurosawa et al. 2012), orange, mandarin and lemon peels (Ghanem et al. 2012) and eggplant (Brasiello et al. 2013). Shrinkage percentage of terebinth fruit (S_b) under different solar drying conditions is presented in the following model:

$$S_b = 6.94v + 18.303,\ R^2 = 0.9917 \quad (17)$$

Most colour changes (ΔR = 22%), ΔG = 25% and ΔB = 20%) were obtained at the air velocity of 1 m/s and min. changes (

R = 9%, ΔG = 5% and ΔB = 14%) achieved at natural airflow (Fig. 9). Results showed that by increasing the airflow velocity, colour changes (ΔRGB) was also increased, so that browning reactions caused more colour change. Arslan and Ozcan (2011) have pointed out this colour change of peppers. These results indicated that higher temperature in hot air convective drying caused more colour change. This in turn led to higher levels of pigment degradation and browning reaction. The colour of dried terebinth seed was more intense, so darker and greener colours are observed when compared to un-treated dry samples. Pott et al. (2005) reported that high temperatures and excessive drying resulted in a noticeable increase in redness in mango slices. Similar results have been obtained in onion (Arslan, Ozcan 2010) and cabbage (Phungamngoen et al. 2013). Relationships between colour changes and air velocity are shown as follows:

$$\Delta R = 3.2v + 10.79,\ R^2 = 0.9997 \quad (18)$$

$$\Delta G = 6.39v + 2.70,\ R^2 = 0.9611 \quad (19)$$

$$\Delta B = 9.94v - 4.56,\ R^2 = 0.9999 \quad (20)$$

Results of the effects of air velocity on rupture force and energy are shown in Fig. 10. The most rupture force and energy values (133.50 N and 1.36 N·m) were achieved at the air velocity of 1 m/s, while the least amounts (122.61 N and 1.07 N·m) were obtained at the natural air flow. Increase in air velocity led to increase in rupture force and energy of terebinth fruit. Firmness is an important indicator determining postharvest quality of fruits and vegetables (Gharibzahedi et al. 2012), which is associated with the cell wall structure of the tissue (Vega-Galvez et al. 2011). The most important postharvest process responsible for degradation of cell wall structure is fruit ripening (Wakabayashi 2000). With increasing and decreasing temperature, the water inside the fruit expands and contracts in volume. This effect is comparable to the effect of turgor pressure. An increased cell tension due to increased turgor or temperature will increase the stiffness and the elastic modulus of the tissue (Hertog et al. 2004; Garcia-Segovia et al. 2010), and this has already been reported in blanched fruits including apple (Johnston et al. 2002), tomato (Hertog et al. 2004) and aloe vera (Vega-Galvez et al. 2011). This could be due to a higher air velocity as terebinth seeds become harder and therefore required more force for cracking. Rupture force and energy of terebinth fruit after drying in the solar dryer were achieved as follows:

$$Fr = 13.15v + 102.84,\ R^2 = 0.9762$$
$$Er = 25.7v + 75.09,\ R^2 = 0.9974 \quad (21)$$

where:

Fr – rupture force (N)

Er – rupture energy (N·m)

doi: 10.17221/45/2013-RAE

CONCLUSION

The effect of solar drying on moisture ratio, drying rate, effective moisture diffusivity, shrinkage, colour, and force and energy rupture of terebinth fruit was investigated. From five thin-layer drying models applied for drying kinetic modelling, the semi-theoretical Logestic model was selected as the best model describing the solar drying behaviour of terebinth fruit. Increasing solar dryer air velocity increased the drying rate and consequently decreased the drying time. The effective moisture diffusivities of terebinth fruit under solar dryer range of natural airflow, 0.5 and 1m/s were in the range of 1.020×10^{-10} to 1.248×10^{-10} m^2/s. Shrinkage percentage increased with increase in air velocity. The highest shrinkage was computed at air velocity of 1 m/s while the lowest was achieved at air velocity of natural airflow. The highest colour change (ΔRGB) was obtained at air velocity of 1 m/s. Maximum and minimim rupture force for the terebinth fruit was 135.62 N and 44.69 N, respectively. Maximum rupture energy was 1.36 N·m. With increasing air temperature, rupture energy was increased. Results revealed that with low cost of assembled solar dryer and two collectors in the opposite directions can be dried high moisture terebinth fruit in a sunny day with high quality.

References

Abbasi Souraki B., Mowla D. (2008): Axial and radial moisture diffusivity in cylindrical fresh green beans in a fluidized bed dryer with energy carrier: modeling with and without shrinkage. Journal of Food Engineering, 88: 9–19.

AOAC (2000): Official methods of analysis of the AOAC. Association of Official Analysis Chemists. Washington DC, USA.

Aghbashlo M., Kianmehr M.H., Hassan-Beygi S.R. (2009): Drying and rehydration characteristics of sour cherry (*Prunuscerasus* L.). Journal of Food Processing and Preservation, 34: 351–365.

Aktas M., Ceylan I., Yilmaz S. (2009): Determination of drying characteristics of apples in a heat pump and solar dryer. Desalination, 239: 266–275.

Altuntas E., Gercekcioglu R., Kaya C. (2010): Selected mechanical and geometric properties of different almond cultivars. International Journal of Food Properties, 13: 282–292.

Amiri Chayjan R., Salari K., Abedi Q., Sabziparvar A.A. (2013): Modeling of moisture diffusivity, activation energy and specific energy consumption of squash seeds in a semi fluidized and fluidized bed drying. Journal of Food Science and Technology, 50: 667–677.

Arevalo-Pinedo A., Murr F.E.X., Arevalo Z.D.S., Giraldo-Zuniga A.D., (2010): Modeling with shrinkage during the vacuum drying of carrot (*Daucuscarota*). Journal of Food Processing and Preservation, 34(S2): 611–621.

Arslan D., Ozcan M.M. (2010): Study the effect of sun, oven and microwave drying on quality of onion slices. LWT-Food Science and Technology, 43: 1121–1127.

Arumuganthan T., Manikantan M.R., Rai R.D., Anandakumar S., Khare V. (2009): Mathematical modeling of drying kinetics of milky mushroom in a fluidized bed dryer. International Agrophysics, 23: 1–7.

Brasiello A., Adiletta G., Russo P., Crescitelli S., Albanese D., Di Matteo M. (2013): Mathematical modeling of eggplant drying: shrinkage effect. Journal of Food Engineering, 114: 99–105.

Cakmak G., Yildiz C. (2011): The drying kinetics of seeded grape in solar dryer with PCM-based solar integrated collector. Food and Bioproduct Processing, 89: 103–108.

Chowdhury M.M.I., Bala B.K., Haquem A. (2011): Energy and exergy analysis of the solar drying of jackfruit leather. Biosystems Engineering, 110: 222–229.

Cihan A., Kahveci K., Hacihafizoglu O. (2007): Modeling of intermittent drying of thin layer rough rice. Journal of Food Engineering, 79: 293–298.

Dash A.K., Pradhan R.C., Das L.M., Naik S.N. (2008): Some physical properties of simarouba fruit and kernel. International Agrophysics, 22: 111–116.

Demir V., Gunhan T., Yagcioglu A.K. (2007): Mathematical modeling of convection drying of green table olives. Biosystems Engineering, 98: 47–53.

Desmorieux H., Madiouli J., Herraud C., Mouaziz H. (2010): Effects of size and form of *Arthrospira spirulina* biomass on the shrinkage and porosity during drying. Journal of Food Engineering, 100: 585–595.

Doymaz I. (2004): Pretreatment effect on sun drying of mulberry fruits (*Morus alba* L.). Journal of Food Engineering, 65: 205–209.

Doymaz I. (2005): Sun drying of figs: an experimental study. Journal of Food Engineering, 71: 403–407.

Garcia-Segovia P., Mognetti C., Andres-Bello A., Martinez-Monzo J. (2010): Osmotic dehydration of Aloe vera (*Aloe barbadensis* Miller). Journal of Food Engineering, 97: 154–160.

Ghanem N., Mihoubi D., Kechaou N., Mihobi N.B. (2012): Microwave dehydration of three citrus peel cultivars: Effect on water and oil retention capacities, color, shrinkage and total phenols content. Industrial Crops and Products, 40: 167–177.

Gharibzahedi S.M.T., Mousavi S.M., Hamedi M., Khodaiyan F., 2012. Comparative analysis of new Persian walnut culti-

doi: 10.17221/45/2013-RAE

vars: nut/kernel geometrical, gravimetrical, frictional and mechanical attributes and kernel chemical composition. Scientia Horticulturae (ISHS), 135: 202–209.

Hashemi G., Mowla D., Kazemeini M. (2009): Moisture diffusivity and shrinkage of broad beans during bulk drying in an inert medium fluidized bed dryer assisted by dielectric heating. Journal of Food Engineering, 92: 331–338.

Hertog A.T.M., Ben-Arie R., Roth E., Nicola B.M. (2004): Humidity and temperature effects on invasive and non-invasive firmness measures. Postharvest Biology and Technology, 33: 79–91.

Hii C.L., Law C.L., Cloke M., Suzannah S. (2009): Thin layer drying kinetics of cocoa and dried product quality. Biosystems Engineering, 102: 153–161.

Hossain M.A., Bala B.K. (2007): Drying of hot chilli using solar tunnel drier. Solar Energy, 81: 85–92.

Janjai S., Mahayothee B., Lamlert N., Bala B.K., Precoppe M., Nagle M., Muller J. (2010): Diffusivity, shrinkage and simulated drying of litchi fruit (*Litchi chinensis* Sonn.). Journal of Food Engineering, 96: 214–221.

Janjai S., Precoppe M., Lamlert N., Mahayothee B., Bala B.K., Nagle M., Muller J. (2011): Thin-layer drying of litchi (*Litchi chinensis* Sonn.). Food and Bioproduct Processing, 89: 194–201.

Janjai S., Lamlert N., Intawee P., Mahayothee B., Bala B.K., Nagle M., Muller J. (2009): Experimental and simulated performance of a PV-ventilated solar greenhouse dryer for drying of peeled longan and banana. Solar Energy, 83: 1550–1565.

Johnston J.W., Hewett E.W., Hertog A.T.M. (2002): Postharvest softening of apple (*Malus domestica*) fruit: a review. Crop and Horticultural Science, 30: 145–160.

Kaya A., Aydin O., Demirtas C. (2007): Drying kinetics of red delicious apple. Biosystems Engineering, 96: 517–524.

Kingsly A.R.P., Meena H.R., Jain R.K., Singh D.B. (2007): Shrinkage of ber (*Zizyphus mauritian* L.) fruits during sun drying. Journal of Food Engineering, 79: 6–10.

Kituu G.M., Shitanda D., Kanali C.L., Mailutha J.T., Njoroge C.K., Wainaina J.K., Silayo V.K. (2010): Thin layer drying model for simulating the drying of Tilapia fish (*Oreochromis niloticus*) in a solar tunnel dryer. Journal of Food Engineering, 98: 325–331.

Koc B., Eren I., Ertekin F.K. (2008): Modelling bulk density, porosity and shrinkage of quince during drying: the effect of drying method. Journal of Food Engineering, 85: 340–349.

Kurosawa L.E., Hubinger M.D., Park K.J. (2012): Glass transition phenomenon on shrinkage of papaya during convective drying. Journal of Food Engineering, 108: 43–50.

Manuwa S.I., Muhammad H.A. (2011): Effects of moisture content and compression axis on mechanical properties of Shea kernel. Journal of Food Engineering, 105: 144–148.

Mercier S., Villeneuve S., Mondor M., Des Marchais L.P. (2011): Evolution of porosity, shrinkage and density of pasta fortified with pea protein concentrate during drying. LWT-Food Science and Technology, 44: 883–890.

Mohsenin N.N. (1996): Physical characteristics: Physical Properties of Plant and Animal Materials. New York, Gordon and Breach Science Publisher.

Nazari Galedar M., Mohtasebi S.S., Tabatabaeefar A., Jafari A., Fadaei H. (2009): Mechanical behavior of pistachio nut and its kernel under compression loading. Journal of Food Engineering, 95: 499–504.

Odjo S., Malumba P., Dossou J., Janas S., Bera F. (2012): Influence of drying and hydrothermal treatment of corn on the denaturation of salt-soluble proteins and color parameters. Journal of Food Engineering, 109: 561–570.

Phungamngoen C., Chiewchan N., Devahastin S. (2013): Effects of various pretreatments and drying methods on *Salmonella* resistance and physical properties of cabbage. Journal of Food Engineering, 115: 237–244.

Pott I., Neidhart S., Muhlbauer W., Carle R. (2005): Quality improvement of non-sulphited mango slices by drying at high temperatures. Innovative of Food Science and Emerging Technology, 6: 412–419.

Prachayawarakorn S., Sawangduanpen S., Saynampheung S., Poolpatarachewin T., Soponronnarit S., Nathakakule A. (2004): Kinetics of colour change during storage of dried garlic slices as affected by relative humidity and temperature. Journal of Food Engineering, 62: 1–7.

Sacilik K., Keskin R., Elicin A.K. (2006): Mathematical modelling of solar tunnel drying of thin layer organic tomato. Journal of Food Engineering, 73: 231–238.

Singh K.P., Mishra H.N., Saha S. (2010): Moisture-dependent properties of barnyard millet grain and kernel. Journal of Food Engineering, 96: 598–606.

Sirisomboon P., Kitchaiya P., Pholpho T., Mahuttanyavanitch W. (2007): Physical and mechanical properties of *Jatropha curcas* L. Fruits, nuts and kernels. Biosystems Engineering, 97: 201–207.

Tripathy P.P., Kumar S. (2009): A methodology for determination of temperature dependent mass transfer coefficients from drying kinetics: Application to solar drying. Journal of Food Engineering, 90: 212–218.

Usub T., Lertsatitthankorn C., Poomsa-Ad N., Wiset L., Siriamornpun S., Soponronnarit S. (2010): Thin layer solar drying characteristics of silkworm pupae. Food and Bioproduct Processing, 88: 149–160.

Vega-Galvez A., Miranda M., Diaz L.P., Lopez L., Rodriguez K., Di Scala K. (2010): Effective moisture diffusivity

doi: 10.17221/45/2013-RAE

determination and mathematical modeling of the drying curves of the olive-waste cake. Bioresource Technology, 101: 7265–7270.

Vega-Galvez A., Uribe E., Perez M., Tabilo-Munizaga G., Vergara J., Garcia-Segovia P., Lara E., Di Scala K. (2011): Effect of high hydrostatic pressure pretreatment on drying kinetics, antioxidant activity, firmness and microstructure of Aloe vera (*Aloe barbadensis* Miller) gel. LWT-Food Science and Technology, 44: 384–391.

Wakabayashi K. (2000): Minireview: changes in cell wall polysaccharides during fruit ripening. Journal of Plant Research, 113: 231–237.

Yadollahinia A., Latifi A., Mahdavi R. (2009): New method for determination of potato slice shrinkage during drying. Computers and Electronics in Agriculture, 65: 268–274.

Zheng C., Sun D.W., Zheng L. (2006): Correlating color to moisture content of large cooked beef joints by computer vision. Journal of Food Engineering, 77: 858–863.

Zielinska M., Markowski M. (2010): Air drying characteristics and moisture diffusivity of carrots. Chemical Engineering and Processing: Process Intensification, 49: 212–218.

Received for publication April 23, 2013
Accepted after corrections January 29, 2014

Corresponding author:

Dr. R. Amiri Chayjan, Bu-Ali Sina University, Faculty of Agriculture, Department of Biosystems Engineering, 6517833131, Hamedan, Iran
phone: + 98 811 442 4366; e-mail: amirireza@basu.ac.ir, amirireza@gmail.com